Interhemispheric Effect of Global Geography on Earth's Climate Response to Orbital Forcing

Rajarshi Roychowdhury[1] and Robert DeConto[1]

[1]University of Massachusetts - Amherst

Correspondence to: rroychowdhur@geo.umass.edu

Postal Address:

Department of Geosciences
627 North Pleasant Street
233 Morrill Science Center
University of Massachusetts
Amherst, MA 01003-9297

Abstract

The climate response of the Earth to orbital forcing shows a distinct hemispheric asymmetry due to the unequal distribution of land in the Northern versus Southern Hemispheres. This asymmetry is examined using a Global Climate Model (GCM) for different climate responses such as Mean Summer Temperatures and Positive Degree Days. A Land Asymmetry Effect (LAE) is quantified for each hemisphere and the results show how changes in obliquity and precession translate into variations in the calculated LAE. We find that the global climate response to specific past orbits is likely unique and modified by complex climate-ocean-

cryosphere interactions that remain poorly known. Nonetheless, these results provide a baseline for interpreting contemporaneous proxy climate data spanning a broad range of latitudes, which maybe useful in paleoclimate data-model comparisons, and individual time-continuous records exhibiting orbital cyclicity.

1. Introduction

The arrangement of continents on the Earth's surface plays a fundamental role in the Earth's climate response to forcing. Due to the asymmetric global geography of the Earth, more continental land area is found in the Northern Hemisphere (68%) as compared to the Southern Hemisphere (32%). These different ratios of land vs. ocean in each hemisphere affect the balance of incoming and outgoing radiation, atmospheric circulation, ocean currents, and the availability of terrain suitable for growing glaciers and ice-sheets. Subsequently, the climate response of the Earth to radiative forcing is asymmetric (Figure 1b and 1c), while the radiative forcing (top-of-atmosphere solar radiation) itself is symmetric across the two hemispheres (Figure 1a). As a result of the inherent land-ocean asymmetry of the Earth, the climatic responses of the Northern and Southern Hemisphere differ for an identical change in radiative forcing (Barron et al., 1984; Deconto et al., 2008; Kang et al., 2014; Short et al., 1991).

Charles Lyell was the first to consider the influence of paleogeography on surface temperatures, in the context of the connection between climate and the modern distribution of land and sea (Lyell, 1832). By comparing the climates of the Northern and Southern Hemispheres and the distribution of land and sea, Lyell pointed out that the present continental distribution lowers high latitude temperatures in both hemispheres. He further pointed out that dominance of ocean in the Southern Hemisphere leads to mild winters and cool summers. Lyell's work is significant

in the context of this paper, because it first sparked the debate of continental forcing versus astronomical forcing of climate.

Since then, a number of classic studies have shown interhemispheric asymmetry in climate response of Northern and Southern Hemispheres. Climate simulations made with coupled atmosphere-ocean GCMs typically show a strong asymmetric response to greenhouse-gas loading, with Northern Hemisphere high latitudes experiencing increased warming compared to Southern Hemisphere high latitudes (Flato and Boer, 2001; Stouffer et al., 1989). GCMs also show that the Northern and Southern Hemispheres respond differently to changes in orbital forcing (e.g. Philander et al., 1996). While the magnitude of insolation changes through each orbital cycle is identical for both hemispheres, the difference in climatic response can be attributed to the fact that Northern Hemisphere is land-dominated while Southern Hemisphere is water dominated (Croll, 1870). This results in a stronger response to orbital forcing in the Northern Hemisphere relative to the Southern Hemisphere.

The distribution of continents and oceans have an important effect on the spatial heterogeneity of the Earth's energy balance, primarily via the differences in albedos and thermal properties of land versus ocean (Trenberth et al., 2009). The latitudinal distribution of land has a dominant effect on zonally averaged net radiation balance due to its influence on planetary albedo and ability to transfer energy to the atmosphere through long-wave radiation, and fluxes of sensible and latent heat. The latitudinal net radiation gradient controls the total poleward heat transport requirement, which is the ultimate driver of winds, and ocean circulation (Stone, 1978). Oceans have a relatively slower response to seasonal changes in insolation due to the higher specific heat of water as compared to land, and mixing in the upper ~10-150 m of the ocean. As a result, in the ocean-dominated Southern Hemisphere, the surface waters suppress extreme temperature swings

66 in the winter and provide the atmosphere with a source of moisture and diabatic heating. In the
67 land-dominated Northern Hemisphere, the lower heat capacity of the land combined with
68 relatively high albedo results in greater seasonality, particularly in the interiors of large
69 continents of Asia and North America. The land surface available in a particular hemisphere
70 also affects the potential for widespread glaciation, and the extreme cold winters associated with
71 large continents covered by winter snow.

72 Continental geography has a strong impact on polar climates, as is evident from the very
73 different climatic regimes of the Arctic and the Antarctic. Several early paleoclimate modeling
74 studies using GCMs investigated continental distribution as a forcing factor of global climate
75 (e.g. Barron et al., 1984; Hay et al., 1990). These studies demonstrated that an Earth with its
76 continents concentrated in the low latitudes is warmer and has lower equator-to-pole temperature
77 gradients than an Earth with only polar continents. Although these early model simulations did
78 not incorporate all the complexities of the climate system, the results provided valuable insights
79 from comparative studies of polar versus equatorial continents in the Earth and showed that
80 changes in continental configuration has significant influence on climatic response to forcing.

81 The asymmetry in the climates of the Northern and Southern Hemispheres can be attributed to
82 three primary causes: (i) Astronomical: Variation in insolation intensity across the Northern and
83 Southern Hemispheres caused by the precession of the equinoxes (today perihelion coincides
84 with January 3, just after the December 21 solstice, leading to slightly stronger summer
85 insolation in the Southern Hemisphere); (ii) Continental geography: the effect of the continental
86 geography on climate as described above; and (iii) Interhemispheric continental geography, i.e.
87 the effect of Northern Hemisphere continental geography on Southern Hemisphere climate and
88 vice-versa. The aim of this study is to gain a better understanding and isolate the effect of

89 interhemispheric continental geography on climate by comparing results from GCM simulations
90 using modern versus idealized (hemispherically symmetric) global geographies. The GCM
91 simulations with modern and idealized (symmetric) geographies are used to quantify the
92 different climate responses to a range of orbits. By comparing the climatic response from
93 simulations with different geographies, we isolate and estimate the effect of interhemispheric
94 continental geography, i.e. the influence of one hemisphere's geography on the climate response
95 of the opposite hemisphere.

96 One of the main caveats of this study is the lack of a dynamical ocean in our model setup. While
97 this presents certain limitations, the model's computational efficiency has the advantage of
98 allowing a wide range of orbital parameter space to be explored. We view the inclusion of a full
99 depth dynamical ocean as a next step, hopefully motivated in part by the results published here.
100 Furthermore, dynamical ocean models introduce an additional level of complexity and model-
101 dependencies that we think are best avoided in this initial study.

102 ## 2. Model

103 ### 2.1 Experimental design

104 General Circulation Models (GCM) have been used extensively to study the importance of
105 geography on the Earth's climate in the past. In this study, we use the latest (2012) version of the
106 Global ENvironmental and Ecological Simulation of Interactive Systems (GENESIS) 3.0 GCM
107 with a slab ocean component (Thompson and Pollard, 1997) rather than a full-depth dynamical
108 ocean (Alder et al., 2011). The slab-ocean predicts sea surface temperatures and ocean heat
109 transport as a function of the local temperature gradient and the zonal fraction of land versus sea
110 at each latitude. While explicit changes in ocean currents and the deep ocean are not represented,

111 the computational efficiency of the slab-ocean version of the GCM allows numerous simulations
112 with idealized global geographies and greatly simplifies interpretations of the sensitivity tests by
113 precluding complications associated with ocean model dependencies. The ocean depth is limited
114 to 50-m (enough to capture the seasonal cycle of the mixed layer). In addition to the atmosphere
115 and slab-ocean, the GCM includes model components representing vegetation, soil, snow, and
116 thermo-dynamic sea ice. The 3-D atmospheric component of the GCM uses an adapted version
117 of the NCAR CCM3 solar and thermal infrared radiation code (Kiehl et al., 1998) and is coupled
118 to the surface components by a land-surface-transfer scheme. In the setup used here, the model
119 atmosphere has a spectral resolution of T31 (~3.75°) with 18 vertical layers. Land-surface
120 components are discretized on a higher resolution 2°x2° grid.

121 The GCM uses various geographical boundary conditions (described below) in 2°x2° and
122 spectral T31 grids for surface and AGCM models, respectively. For each set of experiments, the
123 model is run for 50 years. Spin-up is taken into account, and equilibrium is effectively reached
124 after about 20 years of integration. The results used to calculate interhemispheric effects are
125 averaged over the last 20 years of each simulation. Greenhouse gas mixing ratios are identical in
126 all experiments and set at preindustrial levels with CO_2 set at 280 ppmv, N_2O at 288 ppbv and
127 CH_4 at 800 ppbv. The default values for $CFCl_3$ and CF_2Cl_2 values are set at 0 ppm. The solar
128 constant is maintained at 1367 Wm^{-2}.

129 **2.2 Asymmetric and symmetric Earth geographies**

130 The GCM experiments are divided into three sets: 1) Preindustrial CONTROL 2) NORTH-
131 SYMM and 3) SOUTH-SYMM. The Preindustrial CONTROL experiments use a modern global
132 geography spatially interpolated to the model's 2°x2° surface grid (Koenig et al., 2012). The

133 geography provides the land-ice sheet-ocean mask and land–surface elevations used by the
134 GCM.

135 To simulate the climate of an Earth with meridionally symmetric geographies, we created two
136 sets of land surface boundary conditions: NORTH-SYMM and SOUTH-SYMM. For the
137 NORTH-SYMM experiments, the CONTROL experiment boundary conditions are used to
138 generate a modified GCM surface mask, by reflecting the Northern Hemisphere geography
139 (land-sea-ice mask, topography, vegetation, soil texture) across the equator into the Southern
140 Hemisphere. Similarly, in the experiment SOUTH-SYMM, the land mask and geographic
141 boundary conditions in the Southern Hemisphere are mirrored in the Northern Hemisphere. The
142 NORTH-SYMM and SOUTH-SYMM boundary conditions are shown in Figure 2b and 2c, with
143 the CONTROL (Figure 2a) for comparison.

144 **3. Symmetry (and asymmetry in GCM results)**

145 In the first experimental setup, we run the GCM with modern day orbital configuration, i.e.
146 eccentricity is set at 0.0167, obliquity is set at 23.5° and precession such that perihelion
147 coincides with Southern Hemisphere summer. The radiation at Top-of-Atmosphere is symmetric
148 across both Hemispheres (Figure 3a and 3b). Mean Summer Temperature (ST) is calculated from
149 the GCM as the mean of the average daily temperatures for the summer months in each
150 hemisphere. We define summer by an insolation threshold (325 W/m^2); which accounts for the
151 astronomical positions as well as the phasing of the seasonal cycle of insolation. The zonal
152 averages of ST (calculated at each latitude) demonstrate the inherent asymmetry in the Earth's
153 climate between Northern and Southern Hemispheres, especially evident in the higher latitudes
154 (Figure 3c). Positive Degree Days (PDD) captures the intensity as well as the duration of the
155 melt season, and has been shown to be indicative of ice-sheet response to changes in external

156 forcing. Figure 3d shows the PDD for modern orbit, with zonal averages plotted in the log scale.
157 The asymmetry between the Northern and Southern Hemispheres is captured by the GCM in the
158 calculated PDDs.

159 Next, we maintain the modern orbit to test the effect of meriodionally symmetric continents
160 (Figure 3e-h). Figure 3e and 3f show ST and PDD from a simulation in which the Northern
161 Hemisphere geography is reflected in the Southern Hemisphere (thus making the Earth
162 geographically symmetric). Figure 3g and Figure 3h show ST and PDD from the simulation with
163 symmetric Southern Hemisphere continents. Symmetric continents make the climates of
164 Northern and Southern Hemispheres symmetric (>95%). However, due to the current timing of
165 perihelion with respect to the summer solstices, there remains some minor asymmetry. Using an
166 orbit in which perihelion coincides with equinoxes will make the climate truly symmetrical.

167 ## 4. Modern Orbit Simulations

168 ### 4.1 Effect of Southern Hemisphere (SH) on Northern Hemisphere (NH) climate

169 To estimate the effect of SH continental geography on NH climate, we subtract the NH climate
170 of the NORTH-SYMM simulation (symmetric Northern continents in both hemispheres) from
171 the CONTROL simulation (asymmetric, modern orbit). In these two simulations, the only
172 difference in setup is the Southern Hemispheric continental distribution. Thus the difference in
173 NH climate from the two simulations, if any, can be safely ascribed as the effect of SH
174 continental geography on NH climate. We quantify this interhemispheric effect for ST (for NH)
175 as:

176 $$e_{\widehat{Summer\ Temp}} = \frac{1}{n}\sum_i^n (T_i^{control} - T_i^{north}) \quad \ldots(1)$$

177 Analogous to the effect for ST, the effect for PDD, which we call the "Land Asymmetry Effect"
178 (LAE), is defined as follows:

179 $$LAE_{(NH)} = PDD^{control} - PDD^{north} \quad \ldots(2)$$

180 Where $T_i^{control}$ and $PDD^{control}$ are the mean daily temperature and PDD from the CONTROL
181 simulation, and T_i^{North} and PDD^{North} are the mean daily temperature and PDD from the simulation
182 with the North-symmetric geography (NORTH-SYMM). 'n' is the number of days in the
183 summer months in each hemisphere.

184 **4.2 Effect of Northern Hemisphere (NH) on Southern Hemisphere (SH) climate**

185 Similarly, we estimate the effect of NH continental geography on the SH by subtracting the SH
186 climate of the SOUTH-SYMM simulation (symmetric southern continents in both hemispheres)
187 from the CONTROL simulation (asymmetric, modern orbit). In these two simulations, the
188 differences in SH climate in the CONTROL and SOUTH-SYMM simulations, if any, can be
189 ascribed as the 'effect of NH continental geography on SH climate'. We quantify this
190 interhemispheric effect for ST (for SH) and the LAE as:

191 $$e_{\widehat{Summer\ Temp}} = \frac{1}{n}\sum_i^n (T_i^{control} - T_i^{south}) \quad \ldots(3)$$

192 $$LAE_{SH} = PDD^{control} - PDD^{south} \quad \ldots(4)$$

193 where $T_i^{control}$ and $PDD^{control}$ are the mean daily temperature and PDD from the CONTROL
194 simulation, and T_i^{south} and PDD^{south} are the mean daily temperature and PDD from the simulation
195 with the south-symmetric geography (SOUTH-SYMM).

196 **4.3 Results of Modern Orbit Simulations**

Figure 4a and 4b show the interhemispheric effect of continental geography on ST and PDD respectively. For the Northern Hemisphere, the summer temperatures are calculated when the insolation intensity over the Northern Hemisphere is strongest. The asymmetry in the Southern Hemisphere landmasses leads to weakening of the summer warming over North America and Eurasia (blue shaded regions correspond to cooling). Consequently, summer temperatures over Northern Hemisphere continents are lower by 3-6°C relative to a symmetric Earth. There is a positive warming effect in the North-Atlantic Ocean, and in general the Northern Hemisphere oceans are slightly warmer relative to a symmetric Earth. The general trends in the interhemispheric effect on PDD (LAE) (Figure 4b) mimic those of the summer temperatures (Figure 4a).

For the Southern Hemisphere, the summer temperatures are calculated when the insolation is most intense over the Southern Hemisphere during the year. Southern Hemisphere landmasses, except Antarctica, generally show a cooling response during summer, due to Northern Hemisphere geography. Over Antarctica, summer temperatures are higher in the control simulations than in the symmetric simulations, leading to the inference that there is a warming (increase) in summer temperatures due to interhemispheric effect. Also, the Southern Ocean shows a strong positive temperature effect (warming) relative to a symmetric Earth, although this Southern Ocean response might be different or modified if a full-depth dynamical ocean model were used.

5. Idealized Orbit Simulations

Next, we examine the effect of the opposite hemisphere on the Earth's climate response at extreme obliquities (axial tilt) and idealized precessional configurations (positions of the solstices and equinoxes in relation to the eccentric orbit). The orbital parameters used in these

220 experiments are idealized and do not correspond to a specific time in Earth's history. Rather,
221 they are chosen to provide a useful framework for studying the Earth's climate response to
222 precession and obliquity. HIGH and LOW orbits approximate the highest and lowest obliquity in
223 the last three million years (Berger and Loutre, 1991). NHSP (Northern Hemisphere Summer at
224 Perihelion) and SHSP (Southern Hemisphere Summer at Perihelion) orbits correspond to
225 Northern and austral summers coinciding with perihelion, respectively. The other two
226 precessional configurations considered are EP1 and EP2, with the perihelion coinciding with the
227 equinoxes. For the idealized precession simulations, the obliquity is set at its mean value
228 averaged over the last 3 million years. Eccentricity is set at the same moderate value (mean
229 eccentricity over the last 3 million years) for all simulations. Table 1 summarizes the orbits used
230 in the ensemble of model simulations. Here, we focus only on the LAE, as PDD is a better
231 indicator of air temperature's influence on annual ablation over ice-sheets than summer
232 temperature, since this metric captures both the intensity and duration of the melt season.

233 Changes in precession primarily affect seasonal insolation intensity that is well known to be out-
234 of-phase in both hemispheres (Lyell, 1832). To demonstrate an asymmetry in the climate
235 response to precession, we take the differences between two arbitrarily chosen extremes in the
236 precession cycle (NHSP and SHSP) for both the forcing and the climate response. The forcing
237 (summer energy (J)) calculated at the top of the atmosphere is symmetric across both
238 hemispheres (Figure 5a). The difference in the PDDs ($\Delta PDD_{precession}$) is the Earth's climate
239 response to the combined effect of the two precessional motions (wobbling of the axis of rotation
240 and the slow turning of the orbital ellipse). The climate response ($\Delta PDD_{precession}$) is asymmetric
241 across both hemispheres (Figure 5b). However, when we run the precessional simulations in a

242 Earth with symmetric continents, the climate response to precession is symmetrical (Figure 5c
243 and 5d).

244 In contrast to precession, obliquity alters the seasonality of insolation equally in both
245 hemispheres (Figure 5e). A reduction in the tilt from 24.5° (HIGH) to 22° (LOW) reduces
246 annual insolation by ~17 W/m^2 and summer insolation by ~45 W/m^2 in the high latitudes. In the
247 tropics, summer insolation increases by up to ~5 W/m^2. Loutre et al. (2004) among others
248 predicted that global ice volume changes at the obliquity periods could be interpreted as a
249 response to mean annual insolation and meridional insolation gradients. To demonstrate
250 asymmetry in the climate response to obliquity, we take the differences between the highest and
251 lowest obliquities for both the forcing and the climate response. The difference in the PDDs
252 ($\Delta PDD_{obliquity}$) is the Earth's climate response to changes in tilt. Figure 5f shows $\Delta PDD_{obliquity}$
253 and the zonal averages reveal the asymmetry in the obliquity climate response. The same
254 simulations with North-symmetric Earth (Figure 5g) and South-symmetric Earth (Figure 5h)
255 produce symmetrical climate responses to the obliquity cycle.

256 **5. Results of Idealized Orbit Simulations**

257 The effect of SH continental geography on NH at the idealized orbits is estimated using the same
258 method described above, with the LAE for a given orbit (for NH) calculated as:

259 $$LAE_{(NH)} = PDD_{orbit}^{control} - PDD_{orbit}^{north} \quad \ldots(5)$$

260 Similarly, the effect of NH continental geography on SH at the idealized orbits is estimated using
261 the same method described above, with the LAE for a given orbit (for SH) calculated as:

262 $$LAE_{(SH)} = PDD_{orbit}^{control} - PDD_{orbit}^{south} \quad \ldots(6)$$

Figure 6a shows the spatial variation of LAE when perihelion coincides with Northern Hemisphere summer (NHSP). The Northern Hemisphere landmasses show a strong negative response. In this orbit, the Northern Hemisphere experiences elevated summer insolation, but the response is attenuated by the interhemispheric effect. This dampening effect is greatest in the interiors of the Northern Hemisphere continents. If precession is considered in isolation (i.e. constant obliquity), according to the astronomical theory of climate the Northern Hemisphere should experience 'interglacial' conditions when perihelion coincides with boreal summer. However, because of the interhemispheric effect, interglacial (warm summer) conditions are muted relative to those on a symmetric Earth. During this orbit, the Southern Hemisphere experiences 'glacial' (cold summer) conditions due to the weaker summer insolation. The positive effect in the Southern Hemisphere leads to weaker cooling relative to a symmetric Earth. Thus, when perihelion coincides with Northern Hemisphere summer, the interhemispheric effect dampens the magnitude of 'glacial' versus 'interglacial' conditions in both hemispheres.

Figure 6b shows the spatial variation of LAE when perihelion coincides with Southern Hemisphere summer (SHSP). The Northern Hemisphere continents have a weak positive effect, leading to slightly warmer conditions relative to a symmetric Earth. In this orbit, the southern high latitudes experience intense summer insolation. The positive warming effect amplifies the already warm conditions in the Southern Hemisphere. Figures 6c and 6d show the spatial variation of LAE at the two equinoxes respectively, i.e. when Northern Hemisphere vernal equinox is at perihelion (EP1) and when Northern Hemisphere autumnal equinox is at perihelion (EP2). The LAE is in general weaker at the equinoxes than at the solstices.

At HIGH obliquity, there exists a negative effect on Northern Hemisphere continents (Figure 6e), which mutes the strong insolation intensity during summer months. In the Northern

Hemisphere, as a result of continental asymmetry, a decrease in the equator to pole temperature gradient is observed. A lowering of summer temperatures and temperature gradient due to the interhemispheric effect has a negative impact on the deglaciation trigger associated with HIGH obliquity orbits. Thus the interhemispheric effect would hinder the melting of ice during high-obliquity orbits. In the Southern Hemisphere, the positive interhemispheric effect on PDD over Antarctica and the Southern Ocean leads to overall higher temperatures in the high southern latitudes as compared to a symmetric Earth. Thus, during the high obliquity orbits, positive effect helps deglaciation.

At LOW obliquity, the negative effect over Northern Hemisphere continents is generally less intense (Figure 6f). However, even the modest lowering of summer temperatures caused by the interhemispheric effect would support the growth of ice sheets during low obliquity orbits. The positive effect (warming) in the high Southern latitudes would delay the growth of ice sheets.

6. LAE for orbital cycles

Next, we calculate the LAE for a transition through a precessional cycle. We take two arbitrary end points in the precessional cycle (NHSP and SHSP), and calculate the difference of PDDs between the two simulations ($\Delta PDD_{precession\_cycle}$). The LAE for precessional cycle is therefore calculated as:

$$LAE_{(NH)} = \boldsymbol{\Delta} PDD^{control}_{precession\_cycle} - \boldsymbol{\Delta} PDD^{north}_{precession\_cycle} \quad \ldots(7)$$

$$LAE_{(SH)} = \boldsymbol{\Delta} PDD^{control}_{precession\_cycle} - \boldsymbol{\Delta} PDD^{south}_{precession\_cycle} \quad \ldots(8)$$

The LAE shows a strong negative effect in the Northern Hemisphere (Figure 7a). For the Northern Hemisphere, this transition from SHSP to NHSP equates to a transition from cool to warm climate. The negative interhemispheric effect decreases the ΔPDD in the real Earth, thus

weakening the effect of precession in the Northern Hemisphere. The Southern Hemisphere shows a positive effect on PDD at high latitudes. For the Southern Hemisphere, the transition from SHSP to NHSP equates to a transition from warmer to cooler climate. The positive interhemispheric effect at high latitudes decreases the |ΔPDD| in the real Earth, thus weakening the effect of precessional cycle in the Southern Hemisphere high latitudes.

To calculate the LAE for a transition through the obliquity cycle, we take the highest and lowest obliquities (HIGH and LOW), and calculate the difference of PDDs between the two simulations ($\Delta PDD_{obliquity\_cycle}$).). The LAE for obliquity cycle is therefore calculated as:

$$LAE_{(NH)} = \boldsymbol{\Delta} PDD^{control}_{obliquity\_cycle} - \boldsymbol{\Delta} PDD^{north}_{obliquity\_cycle} \quad \ldots(9)$$

$$LAE_{(SH)} = \boldsymbol{\Delta} PDD^{control}_{obliquity\_cycle} - \boldsymbol{\Delta} PDD^{south}_{obliquity\_cycle} \quad \ldots(10)$$

The Northern Hemisphere shows a small negative effect in the high latitudes, and a positive effect in the low latitudes (Figure 7b). The transition from LOW to HIGH corresponds to a transition from cold to warm climate. The negative interhemispheric effect decreases the ΔPDD, thus weakening the climate response of obliquity cycle in the high latitudes. The positive interhemispheric effect increases the ΔPDD, thus strengthening the climate response of obliquity cycle in the low latitudes in the Northern Hemisphere. The Southern Hemisphere shows largely a negative effect, with a positive effect in the high latitudes. The transition from LOW to HIGH corresponds to a transition from cold to warm climate. The positive interhemispheric effect increases the ΔPDD, thus amplifying the effect of obliquity over Antarctica.

6. Correlations between LAE and various climatological variables

A comprehensive, mechanistic evaluation of the hemispheric effect is beyond the scope of this initial study. However, as a first step, we test the relationship between the hemispheric LAE and

various atmospheric processes by exploring correlations between the inter hemispheric responses to orbital forcing, and climatological fields related to changes in radiation (clouds), dynamics (heat and moisture convergence), and feedbacks related to surface processes (particularly sea ice and snow albedo).

Total cloud amount, and liquid water content are used to calculate the "Cloud Effect" (Figure 8a and 8b), in a similar way as the calculation of LAE. At latitudes above 60º, the "Cloud Effect" shows a strong, positive correlation with the LAE (Figure 9a and 9b). Here, the increased cloud cover causes a net warming, also demonstrated by the strong positive correlation in net long wave radiation in the same latitudes (Figure 9c). In the tropics, where mean annual insolation intensity is higher, we find a negative correlation between the "Cloud Effect" and LAE, with increased cloud amounts impacting short-wave absorption via their impact on albedo.

Fractional snow cover and snow thickness also show a strong negative correlation everywhere except Northern Asia. The negative correlation between the snow cover and the LAE is related to an increase in surface albedo, especially in spring and over land surfaces covered by tundra. The correlation is weaker in heavily forested regions, where the snow-albedo feedback is less effective (Bonan et al., 1992). Similarly, fractional sea ice cover (Figure 9f) also shows a negative correlation with the LAE, where increased albedo reduces net shortwave radiative flux.

Next, spatial patterns in the LAE are compared with basic dynamical effects of the different geographies. Sea level pressure clearly shows a response to hemispheric asymmetry (Figure 8g), with a general increase in the Northern Hemisphere and a decrease in Southern Hemisphere. The resulting persistent change in the wind field can be seen in northward winds (Figure 8h) and their correlations with the LAE, implying a dynamical contribution to the LAE anomaly patterns via warm air advection. Spatial patterns in these dynamical linkages can help explain some of the

353 regional anomalies seen in the LAE. For example, we find reduced winds in the North Atlantic
354 leading to reduced heat loss out of that region. This hints at a tropical teleconnection to the
355 westerlies (e.g., Hou et al., 1997), propagating the impact of low latitude geography to the mid
356 latitudes of the opposite hemisphere, in this case with an impact on sea ice and regional warming
357 in the North Atlantic. As expected, we also see a strong positive correlation between the LAE
358 and 500-hPa geopotential height (Figure 9i), whereby a positive "Z500 effect" indicates that the
359 geopotential heights are regionally higher (implying warm temperatures across the region) when
360 compared to a symmetric Earth, and vice-versa. Interhemispheric teleconnections like these have
361 been studied extensively with respect to present day continental geography (Chiang and
362 Friedman, 2012; Harnack and Harnack, 1985; Hou and Hou, 1998; Ji et al., 2014, etc.).
363 However, far field effects such as those arising from interactions between the Hadley circulation
364 and planetary waves (among other dynamical processes) are not adequately resolved at the
365 relatively coarse spatial resolution used in these initial simulations, with monthly meteorological
366 output. A more complete dynamical analysis of the LAE is the subject of ongoing work and a
367 future manuscript.

368 **7. Conclusions**

369 The unbalanced fraction of land in the Northern versus Southern Hemisphere has remained
370 almost unchanged for tens of millions of years. However, the significance of this continental
371 asymmetry on Earth's climate response to forcing has not been previously quantified with a
372 physically based climate models. We find that continental geography of the opposite hemisphere
373 has a control on the climate system's response to insolation forcing, and this may help explain
374 the non-linear response of the Earth's climate to insolation forcing.

According to classical Milankovitch theory, the growth of polar ice sheets at the onset of glaciation requires cooler summers in the high latitudes, in order for snow to persist throughout the year. During warm summers at the high latitudes, the winter snowpack melts, inhibiting glaciation or leading to deglaciation if ice sheets already exist. Thus, the intensity of summer insolation at high latitudes, especially the Northern polar latitudes, has been considered the key driver of the glacial-interglacial cycles and other long-term climatic variations. At precessional periods, at which the high latitude summer insolation intensity primarily varies (Huybers, 2006; Raymo et al., 2006, etc.), the land asymmetry effect plays an important role by amplifying (and weakening at certain times) the effect of summer insolation intensity.

In all the orbital configurations simulated here, we find that the geography of the Southern Hemisphere weakens the temperature response of the high Northern Hemisphere latitudes to orbital forcing. Consequently, this leads to a larger latitudinal gradient in summer temperatures in the Northern Hemisphere compared to that of a symmetric Earth. In particular, the amplification (or weakening) of the response to insolation changes at precessional and obliquity periods might explain some of the important features of late Pliocene-early Pleistocene climate variability, when obliquity-paced cyclicity dominated precession in global benthic $\delta^{18}O$ records. In Figure 7, we have demonstrated that the interhemispheric effect causes a suppression of the effects of precessional cycle on the Earth's surface. In other words, the real Earth has a smaller response to a precession cycle as compared to the hypothetical symmetric Earth. We have also showed that the interhemispheric effect causes an amplification of the effects of obliquity cycle on the Earth's surface. In other words, the real Earth has a larger response to the obliquity cycle in the ocean dominated Southern Hemisphere, as compared to the hypothetical symmetric Earth. Consequently, the interhemispheric effect of continental geography contributes to the muting of

precessional signal and amplification of obliquity signal recorded in paleoclimate proxies such as benthic $\delta^{18}O$ isotope records.

There are various ways in which the Earth's continental asymmetry affects climate. Here, we have shown how these interhemispheric effects influence the Earth's climate response to orbital forcing via the radiative and atmospheric dynamical processes represented in a slab-ocean GCM. While computationally challenging, future work should include complimentary simulations with AOGCMs, to explore the potential modifying role of ocean dynamics on the amplifying and weakening interhemispheric responses to orbital forcing demonstrated here.

406 **Table 1. Experimental Setup of Model Boundary Conditions and Forcings**

Run ID	LSX Configuration	Eccentricity	Obliquity	Precession [a]	GHGs
$CONTROL_{NHSP}$	Modern	0.034	23.2735	270° (NHSP)	Preindustrial
$CONTROL_{SHSP}$	Modern	0.034	23.2735	90° (SHSP)	Preindustrial
$CONTROL_{EP1}$	Modern	0.034	23.2735	0° (EP1)	Preindustrial
$CONTROL_{EP2}$	Modern	0.034	23.2735	180° (EP2)	Preindustrial
$CONTROL_{HIGH}$	Modern	0.034	24.5044	180°	Preindustrial
$CONTROL_{LOW}$	Modern	0.034	22.0425	180°	Preindustrial
NORTH-$SYMM_{NHSP}$	North-symmetric	0.034	23.2735	270° (NHSP)	Preindustrial
NORTH-$SYMM_{SHSP}$	North-symmetric	0.034	23.2735	90° (SHSP)	Preindustrial
NORTH-$SYMM_{EP1}$	North-symmetric	0.034	23.2735	0° (EP1)	Preindustrial
NORTH-$SYMM_{EP2}$	North-symmetric	0.034	23.2735	180° (EP2)	Preindustrial
NORTH-$SYMM_{HIGH}$	North-symmetric	0.034	24.5044	180°	Preindustrial
NORTH-$SYMM_{LOW}$	North-symmetric	0.034	22.0425	180°	Preindustrial
SOUTH-$SYMM_{NHSP}$	South-symmetric	0.034	23.2735	270° (NHSP)	Preindustrial
SOUTH-$SYMM_{SHSP}$	South-symmetric	0.034	23.2735	90° (SHSP)	Preindustrial
SOUTH-$SYMM_{EP1}$	South-symmetric	0.034	23.2735	0° (EP1)	Preindustrial
SOUTH-$SYMM_{EP2}$	South-symmetric	0.034	23.2735	180° (EP2)	Preindustrial
SOUTH-$SYMM_{HIGH}$	South-symmetric	0.034	24.5044	180°	Preindustrial
SOUTH-$SYMM_{LOW}$	South-symmetric	0.034	22.0425	180°	Preindustrial

407 **NHSP:** Northern Hemisphere Summer Solstice at Perihelion

408 **SHSP:** Southern Hemisphere Summer Solstice at Perihelion

409 **EP1:** Northern Hemisphere Vernal Equinox at Perihelion

410 **EP2:** Northern Hemisphere Autumnal Equinox at Perihelion

411 [a] Orbital precession in the GCM is defined here as the prograde angle from perihelion to the

412 Northern Hemispheric vernal equinox.

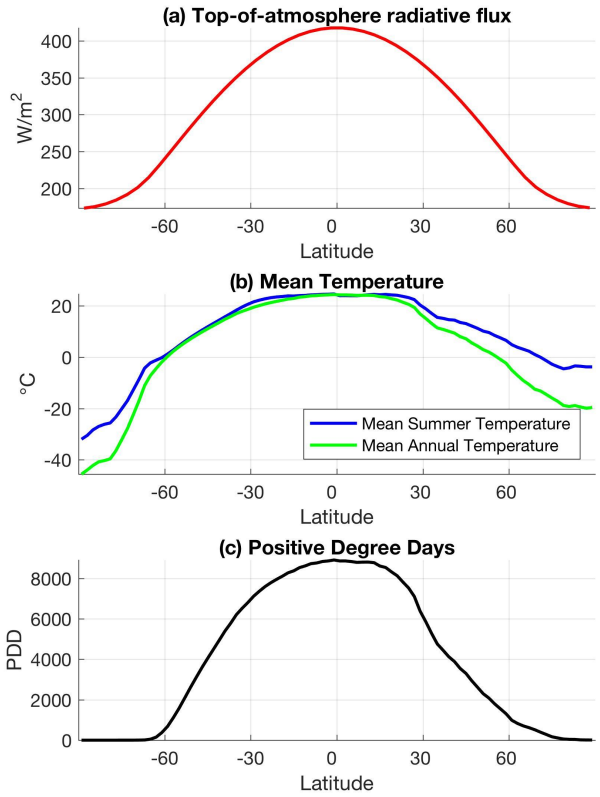

413

414 **Figure 1:** (a) Top-of-atmosphere net incoming radiation (red). (b) Mean Summer Temperatures
415 (blue) and Mean Annual Temperatures (green), computer from GCM simulations with a modern
416 orbit (c) Positive Degree Days (PDD) calculated from GCM simulations with a modern orbit.

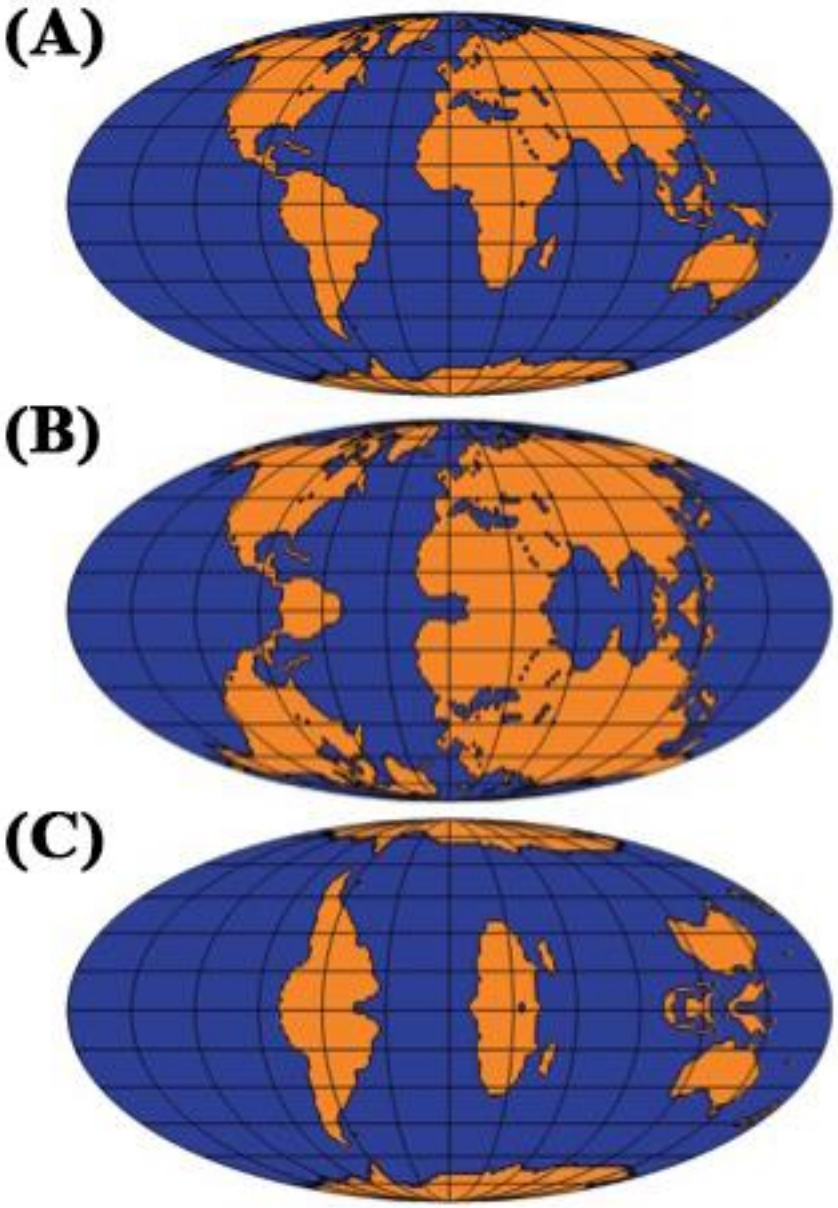

417

418 **Figure 2:** (A) Modern continental geography (B) NORTH-SYMM geography and (C) SOUTH-

419 SYMM geography

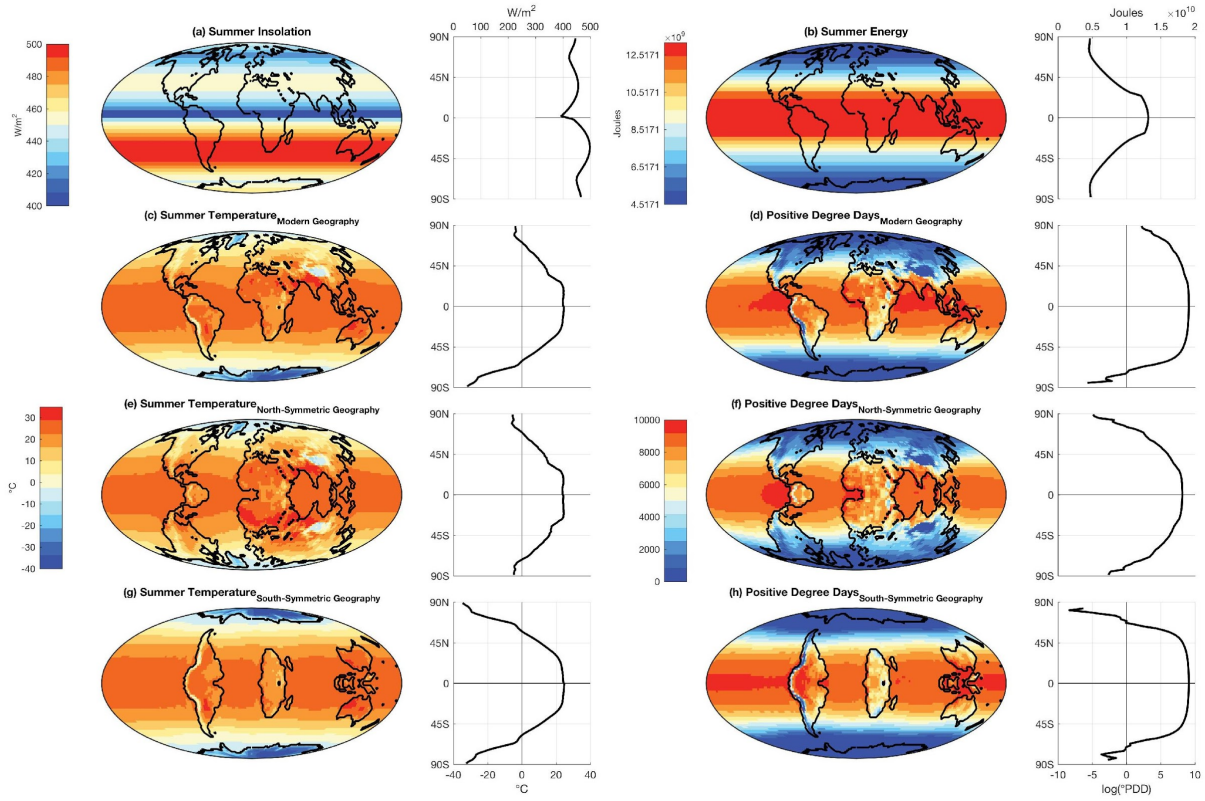

420

421 **Figure 3:** (a-d) Demonstration of Earth's asymmetric climate response to symmetric climate
422 forcing. Simulations are forced with modern orbit: (a) Summer insolation; (b) summer energy;
423 (c) Summer Temperature; and (d) PDD. (e-h) Demonstration of Earth's symmetric climate
424 response to climate forcing when idealized symmetric Earth geographies are used. Simulations
425 are forced by modern day orbit: (e) and (f) Summer Temperature and PDD for NORTH-SYMM
426 simulation, (g) and (h) Summer Temperature and PDD for SOUTH-SYMM simulation. The
427 zonal averages are plotted on the right of each Figure. Zonal averages of PDD are plotted on a
428 log scale.

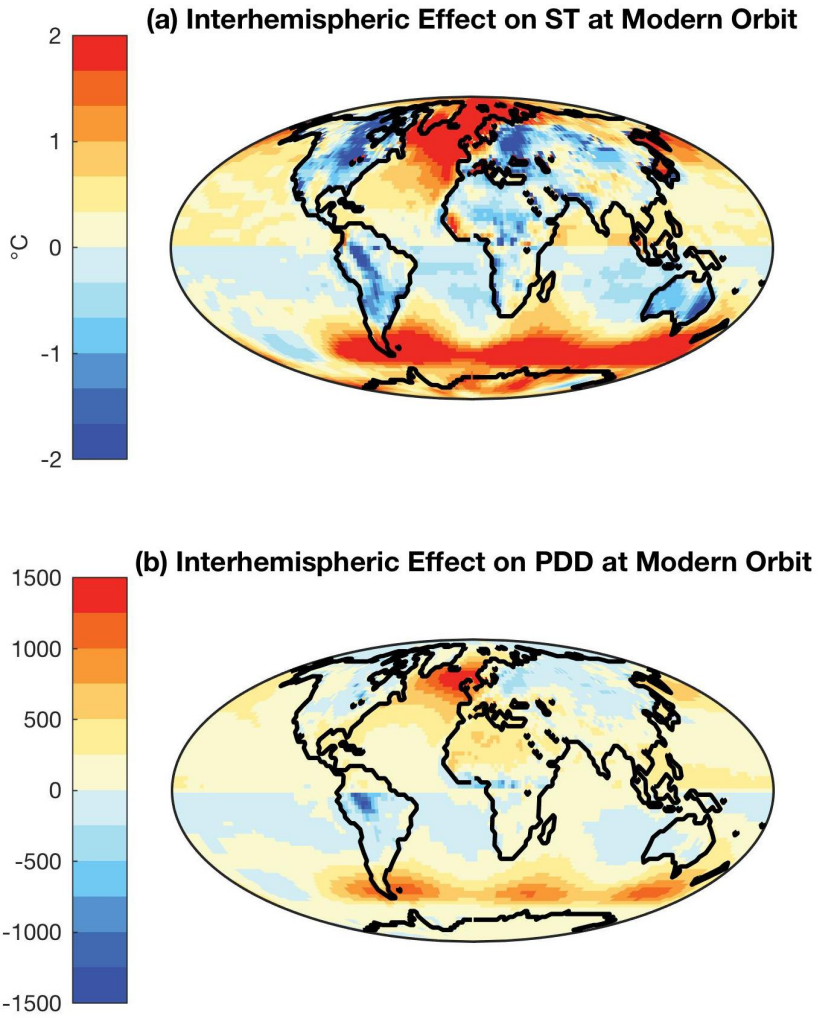

429

430 **Figure 4:** Interhemispheric effect of continental geography (LAE) on: (a) Mean Summer

431 Temperature (ST) and (b) Positive Degree Days (PDD).

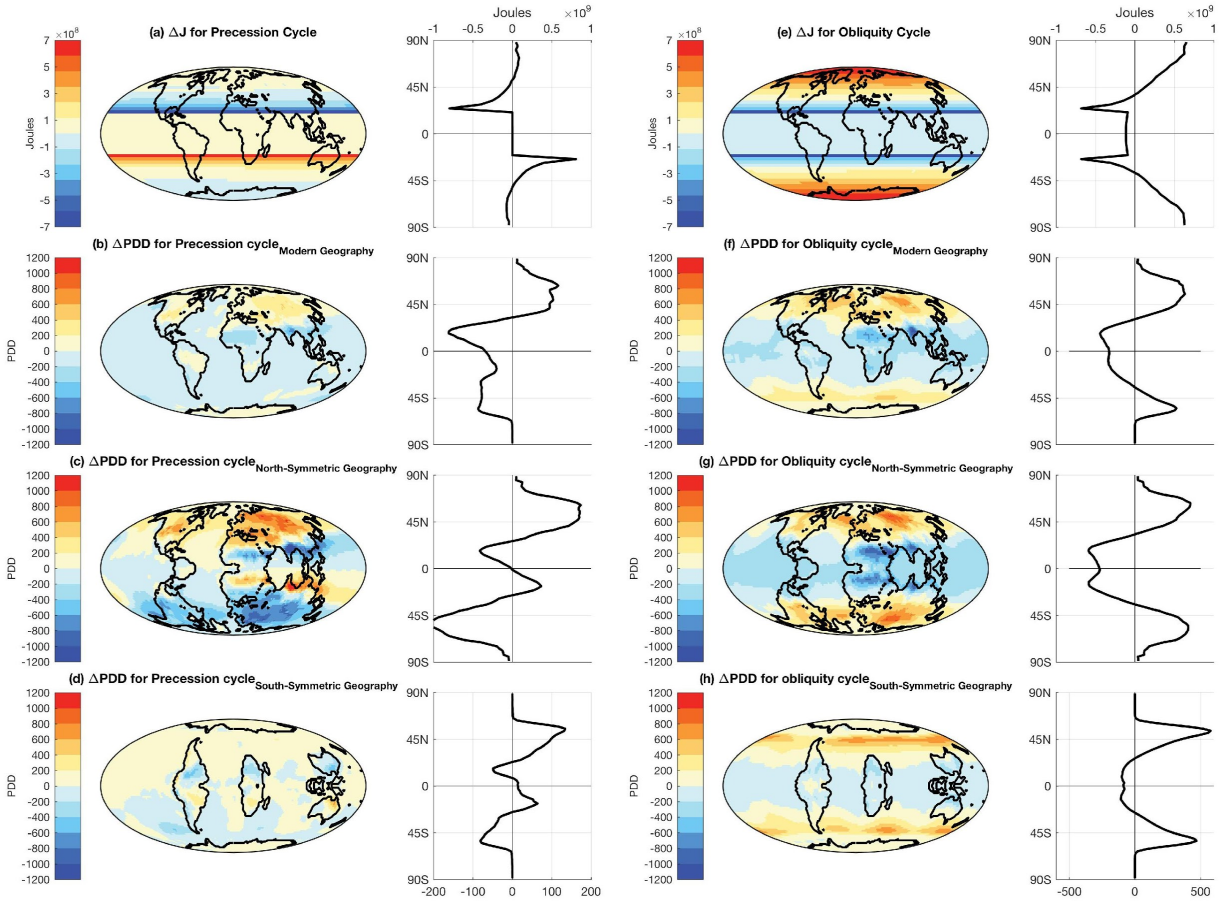

Figure 5: Summer Energy (J) change for a transition from SHSP to NHSP orbit (a); and the corresponding change in Positive Degree Days (PDD) in CONTROL (b); NORTH-SYMM (c) and SOUTH-SYMM (d) simulations. Summer Energy (J) change for a transition from LOW to HIGH orbit (e); and the corresponding change in PDD in CONTROL (f); NORTH-SYMM (g) and SOUTH-SYMM (h) simulations.

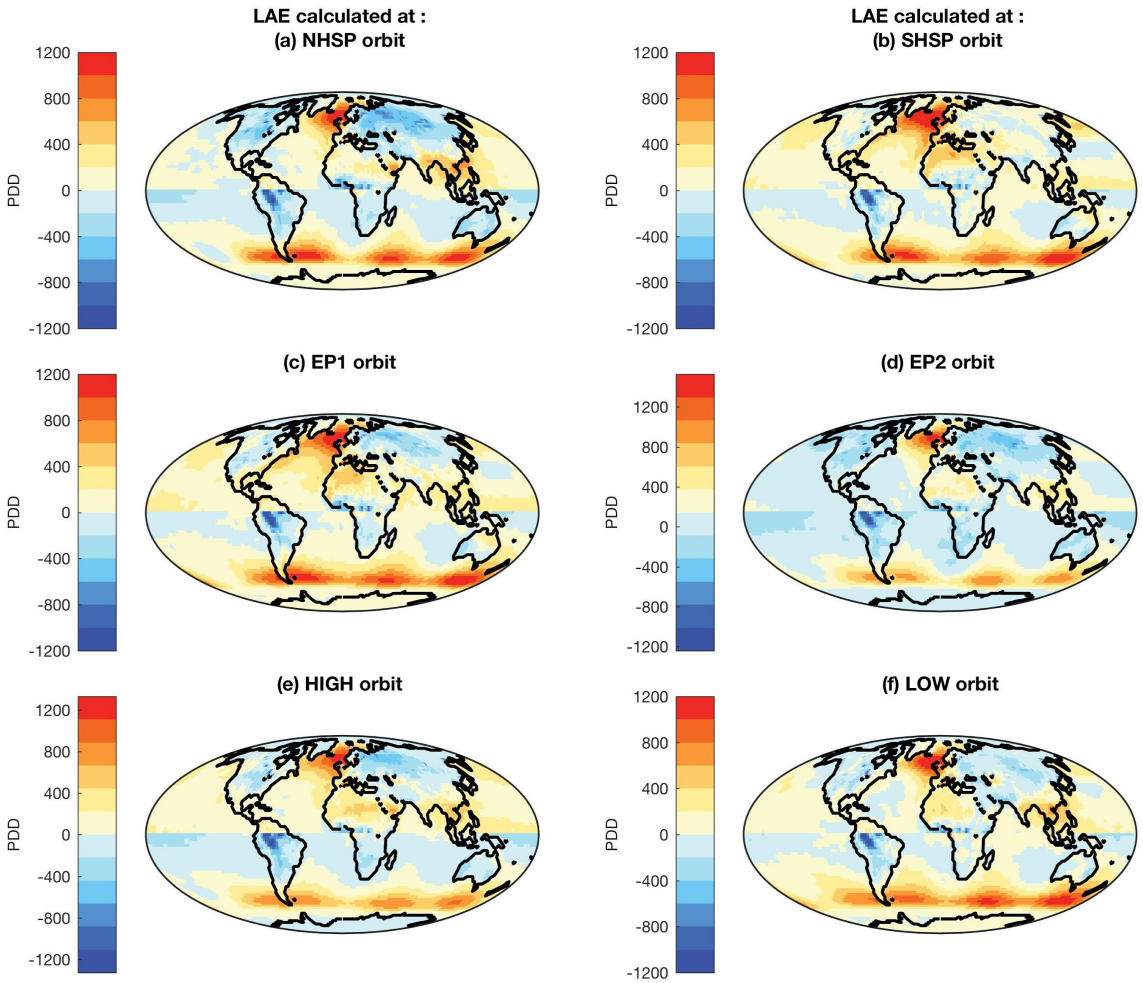

438

439 **Figure 6:** Interhemispheric effect of continental geography (LAE) on the climate response
440 (PDD) at: (a) Northern Hemisphere summer at perihelion; (b) Southern Hemisphere summer at
441 perihelion; (C) Northern Hemisphere vernal equinox at perihelion; (d) Northern Hemisphere
442 autumnal equinox at perihelion; (e) High obliquity orbit; and (f) Low obliquity orbit.

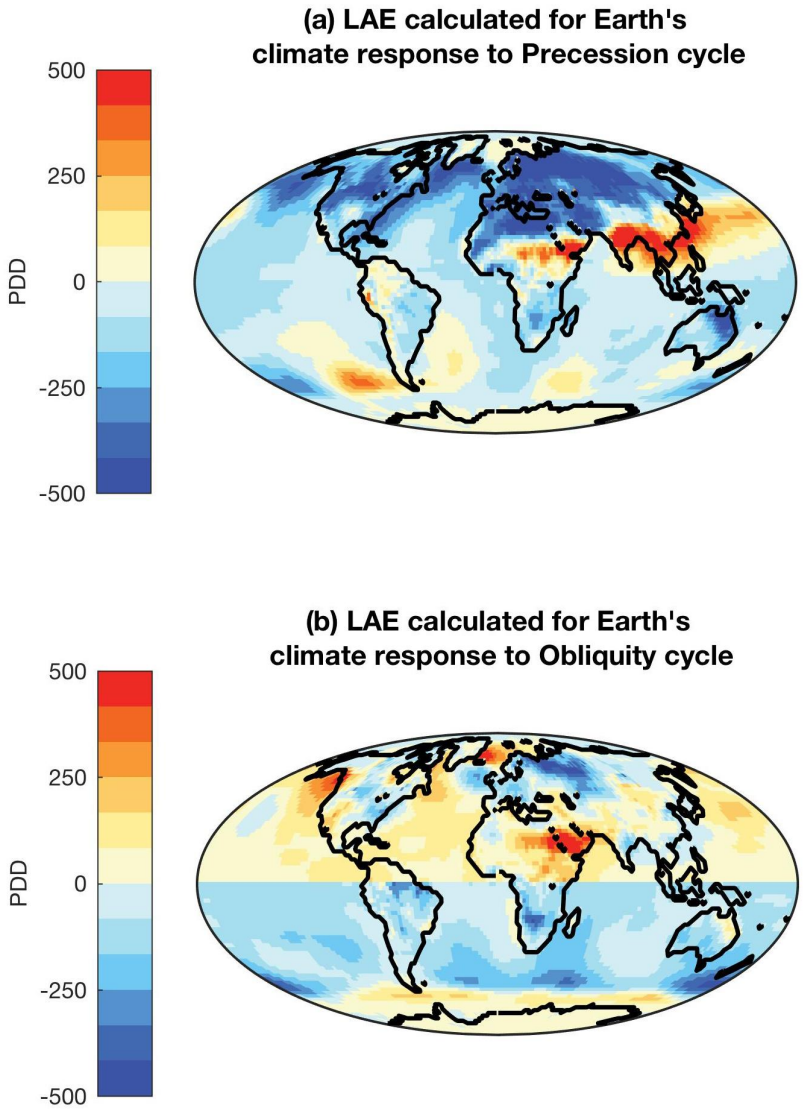

443

444 **Figure 7:** Interhemispheric effect of continental geography on the climate response to: (a)

445 precession cycle (SHSP to NHSP); and (b) obliquity cycle (Low to High).

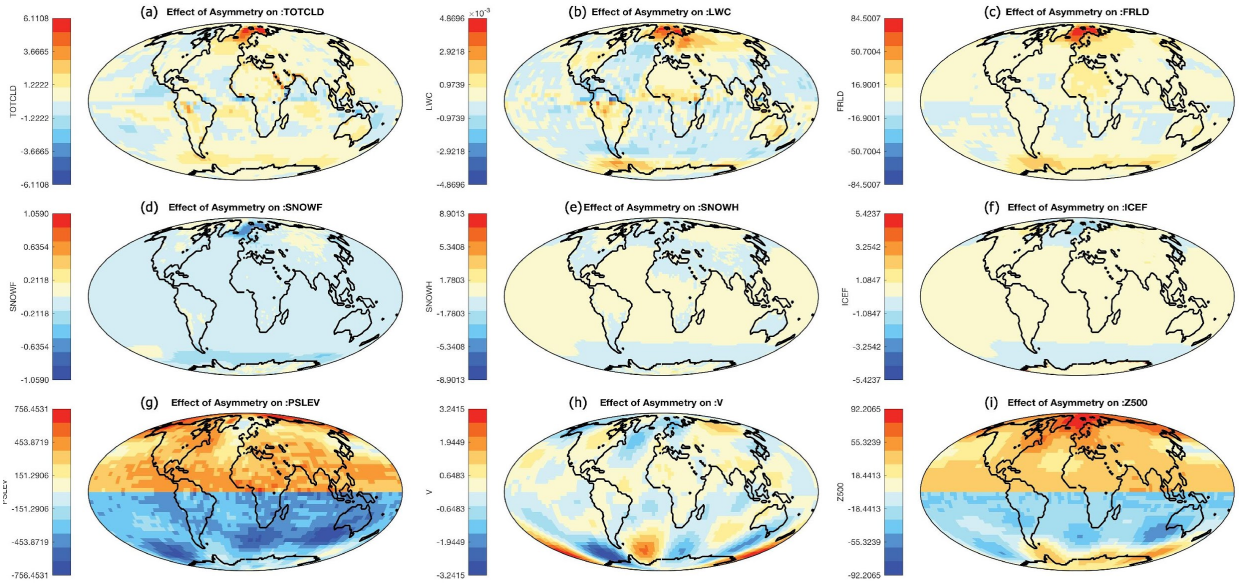

Figure 8: The effect of interhemispheric continental distribution on: (a) Total cloud content (b) Liquid water content (c) Infrared flux absorbed by the surface (d) Fractional snow cover (e) Snow thickness (f) Fractional sea ice cover (g) Sea level pressure (h) Northward wind (i) 500 hPa geopotential height.

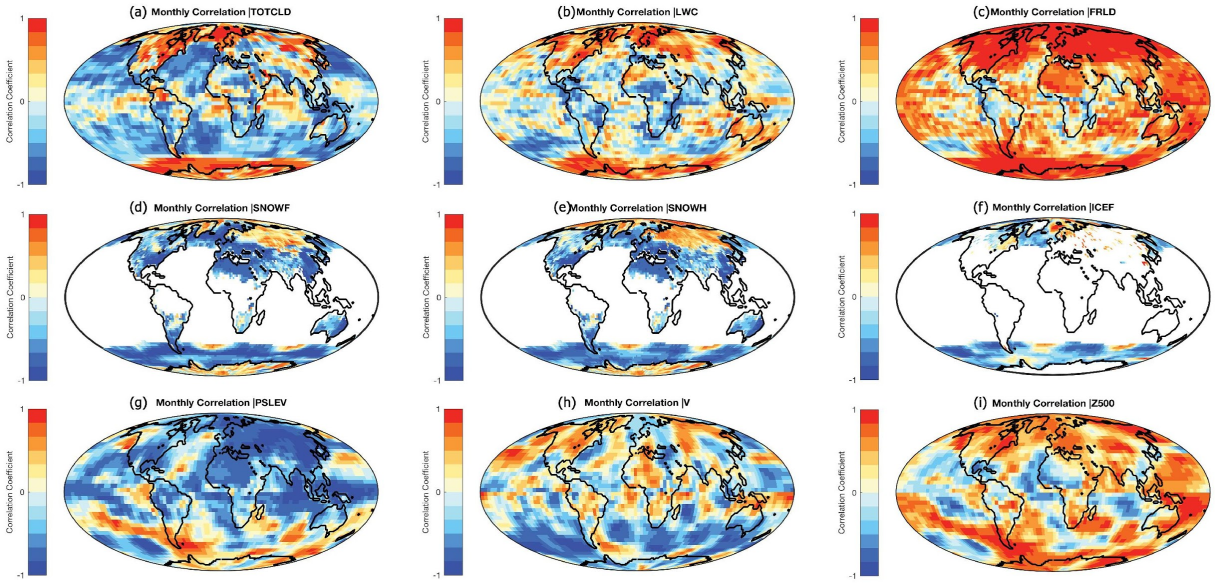

451

452 **Figure 9:** Correlation between LAE and the effect of interhemispheric continental distribution
453 on: (a) Total cloud content (b) Liquid water content (c) Infrared flux absorbed by the surface (d)
454 Fractional snow cover (e) Snow thickness (f) Fractional sea ice cover (g) Sea level pressure (h)
455 Northward wind (i) 500 hPa geopotential height.

Alder, J. R., Hostetler, S. W., Pollard, D. and Schmittner, A.: Evaluation of a present-day climate simulation with a new coupled atmosphere-ocean model GENMOM, Geosci. Model Dev., 4(1), 69–83, doi:10.5194/gmd-4-69-2011, 2011.

Barron, E. J., Thompson, S. L. and Hay, W. W.: Continental distribution as a forcing factor for global-scale temperature, Nature, 310(5978), 574–575, doi:10.1038/310574a0, 1984.

Berger, A. and Loutre, M. F.: Insolation values for the climate of the last 10 million years, Quat. Sci. Rev., 10(4), 297–317, doi:10.1016/0277-3791(91)90033-Q, 1991.

Bonan, G. B., Pollard, D. and Thompson, S. L.: Effects of boreal forest vegetation on global climate, Nature, 359(6397), 716–718, doi:10.1038/359716a0, 1992.

Charles Lyell: Principles of Geology, John Murray: Albemarle Street, London. [online] Available from: https://www.bl.uk/collection-items/charles-lyells-principles-of-geology# (Accessed 31 January 2018), 1832.

Chiang, J. C. H. and Friedman, A. R.: Extratropical Cooling, Interhemispheric Thermal Gradients, and Tropical Climate Change, Annu. Rev. Earth Planet. Sci., 40(1), 383–412, doi:10.1146/annurev-earth-042711-105545, 2012.

Croll, J.: On ocean-currents, part I: ocean-currents in relation to the distribution of heat over the globe., Philos. Mag. J. Sci., 39(259), 81–106, 1870.

Deconto, R. M., Pollard, D., Wilson, P. A., Pälike, H., Lear, C. H. and Pagani, M.: Thresholds for Cenozoic bipolar glaciation., Nature, 455(7213), 652–6, doi:10.1038/nature07337, 2008.

Flato, G. M. and Boer, G. J.: Warming asymmetry in climate change simulations, Geophys. Res. Lett., 28(1), 195–198, doi:10.1029/2000GL012121, 2001.

Harnack, R. P. and Harnack, J.: Intra- and inter-hemispheric teleconnections using seasonal southern hemisphere sea level pressure, J. Climatol., 5(3), 283–296, doi:10.1002/joc.3370050305, 1985.

Hay, W. W., Barron, E. J. and Thompson, S. L.: Results of global atmospheric circulation experiments on an Earth with a meridional pole-to- pole continent, J. Geol. Soc. London., 147(2), 385–392, doi:10.1144/gsjgs.147.2.0385, 1990.

Hou, A. Y. and Hou, A. Y.: Hadley Circulation as a Modulator of the Extratropical Climate, J. Atmos. Sci., 55(14), 2437–2457, doi:10.1175/1520-0469(1998)055<2437:HCAAMO>2.0.CO;2, 1998.

Huybers, P.: Early Pleistocene glacial cycles and the integrated summer insolation forcing., Science, 313(5786), 508–11, doi:10.1126/science.1125249, 2006.

Ji, X., Neelin, J. D., Lee, S.-K., Mechoso, C. R., Ji, X., Neelin, J. D., Lee, S.-K. and Mechoso, C. R.: Interhemispheric Teleconnections from Tropical Heat Sources in Intermediate and Simple Models, J. Clim., 27(2), 684–697, doi:10.1175/JCLI-D-13-00017.1, 2014.

Kang, S. M., Seager, R., Frierson, D. M. W. and Liu, X.: Croll revisited: Why is the northern hemisphere warmer than the southern hemisphere?, Clim. Dyn., 1457–1472, doi:10.1007/s00382-014-2147-z, 2014.

Kiehl, J. T., Hack, J. J., Bonan, G. B., Boville, B. a., Williamson, D. L. and Rasch, P. J.: The National Center for Atmospheric Research Community Climate Model: CCM3*, J. Clim., 11(6), 1131–1149, doi:10.1175/1520-0442(1998)011<1131:TNCFAR>2.0.CO;2, 1998.

Koenig, S. J., DeConto, R. M. and Pollard, D.: Pliocene Model Intercomparison Project

Experiment 1: implementation strategy and mid-Pliocene global climatology using GENESIS v3.0 GCM, Geosci. Model Dev., 5(1), 73–85, doi:10.5194/gmd-5-73-2012, 2012.

Loutre, M.-F., Paillard, D., Vimeux, F. and Cortijo, E.: Does mean annual insolation have the potential to change the climate?, Earth Planet. Sci. Lett., 221(1–4), 1–14, doi:10.1016/S0012-821X(04)00108-6, 2004.

OHBA, M. and UEDA, H.: A GCM Study on Effects of Continental Drift on Tropical Climate at the Early and Late Cretaceous, J. Meteorol. Soc. Japan, 88(6), 869–881, doi:10.2151/jmsj.2010-601, 2010.

Philander, S. G. H., Gu, D., Lambert, G., Li, T., Halpern, D., Lau, N.-C. and Pacanowski, R. C.: Why the ITCZ Is Mostly North of the Equator, J. Clim., 9(12), 2958–2972, doi:10.1175/1520-0442(1996)009<2958:WTIIMN>2.0.CO;2, 1996.

Poulsen, C. J., Barron, E. J., Johnson, C. C. and Fawcett, P.: Links between major climatic factors and regional oceanic circulation in the Mid-Cretaceous, in Special Paper 332: Evolution of the Cretaceous Ocean-Climate System, pp. 73–89, Geological Society of America., 1999.

Raymo, M. E., Lisiecki, L. E. and Nisancioglu, K. H.: Plio-Pleistocene Ice Volume, Antarctic Climate, and the Global d18O Record, , 313(July), 492–495, 2006.

Short, D. A., Mengel, J. G., Crowley, T. J., Hyde, W. T. and North, G. R.: Filtering of Milankovitch Cycles by Earth's Geography, Quat. Res., 35(2), 157–173, doi:10.1016/0033-5894(91)90064-C, 1991.

Stone, P. H.: Constraints on dynamical transports of energy on a spherical planet, Dyn. Atmos. Ocean., 2(2), 123–139, doi:10.1016/0377-0265(78)90006-4, 1978.

519 Stouffer, R. J., Manabe, S. and Bryan, K.: Interhemispheric asymmetry in climate response to a
520 gradual increase of atmospheric CO2, Nature, 342(6250), 660–662, doi:10.1038/342660a0,
521 1989.

522 Thompson, S. L. and Pollard, D.: Greenland and Antarctic Mass Balances for Present and
523 Doubled Atmospheric CO 2 from the GENESIS Version-2 Global Climate Model, J. Clim.,
524 10(5), 871–900, doi:10.1175/1520-0442(1997)010<0871:GAAMBF>2.0.CO;2, 1997.

525 Trenberth, K. E., Fasullo, J. T., Kiehl, J., Trenberth, K. E., Fasullo, J. T. and Kiehl, J.: Earth's
526 Global Energy Budget, Bull. Am. Meteorol. Soc., 90(3), 311–323,
527 doi:10.1175/2008BAMS2634.1, 2009.